
Self-Training Ensemble Networks for Zero-Shot Image Recognition

Meng Ye

Computer and Information Science
Temple University, Philadelphia, USA
meng.ye@temple.edu

Yuhong Guo

School of Computer Science
Carleton University, Ottawa, Canada
yuhong.guo@carleton.ca

Abstract

Despite the advancement of supervised image recognition algorithms, their dependence on the availability of labeled data and the rapid expansion of image categories raise the significant challenge of zero-shot learning. Zero-shot learning (ZSL) aims to transfer knowledge from labeled classes into unlabeled classes to reduce human labeling effort. In this paper, we propose a novel self-training ensemble network model to address zero-shot image recognition. The ensemble network is built by learning multiple image classification functions with a shared feature extraction network but different label embedding representations, each of which facilitates information transfer to different subsets of unlabeled classes. A self-training framework is then deployed to iteratively label the most confident images in each unlabeled class with predicted pseudo-labels and update the ensemble network with the training data augmented by the pseudo-labels. The proposed model performs training on both labeled and unlabeled data. It can naturally bridge the domain shift problem in visual appearances and be extended to the generalized zero-shot learning scenario. We conduct experiments on multiple standard ZSL datasets and the empirical results demonstrate the efficacy of the proposed model.

1 Introduction

Despite the effectiveness of deep convolutional neural networks (CNNs) on supervised image classification problems, zero shot learning (ZSL) remains a challenging and fundamental problem due to the rapid expansion of image categories and the lacking in labeled training data. As a special unsupervised domain adaptation, ZSL aims to transfer information from the source domain, a set of training classes with labeled data, to make predictions in the target domain, a set of test classes with only unlabeled data. Different from standard domain adaptation, in ZSL the labeled training classes and unlabeled test classes have no overlaps – they are entirely disjoint. Based on the visibility of the instance labels, the training classes and the test classes are usually referred to as *seen* and *unseen* classes respectively.

Existing zero-shot image recognitions have centered on deploying label embeddings in a common semantic space, e.g., in terms of high level visual attributes, to bridge the domain gap between *seen* and *unseen* classes. For example, animals share some common characteristics such as ‘black’, ‘yellow’, ‘spots’, ‘stripes’ and so on. Thus each animal class, either seen or unseen, can be represented as a binary vector in the semantic attribute space, with each element denoting the appearance/absence of certain attribute. Much ZSL effort in this direction has focused on developing effective mapping models from the input visual feature space to the semantic label embedding space [23, 10, 5, 19], or learning suitable compatibility functions between the two spaces [2, 26, 30], to facilitate prediction information transfer from the seen classes to the unseen classes. However, these methods identify visual-semantic mappings only on the labeled seen class data, which poses a fundamental *domain*

shift problem due to the appearance variations of visual attributes across *seen* and *unseen* classes, and has negative impact on cross-class generalization (i.e., ZSL performance) [11, 18].

In this paper, we propose a novel self-training ZSL framework with an ensemble network to address the domain shift problem and improve the generalization ability of ZSL. Existing ZSL works rely on a single set of label embeddings to build inter-class label relations for knowledge transfer, which can hardly be suitable for all the unseen classes. Instead we construct a deep ensemble network that consists of multiple image classification functions with a shared feature extraction convolutional neural network and different label embedding representations. Each label embedding representation is optimized to facilitate information transfer from the seen classes to only a subset of unseen classes. By exploiting multiple classifiers in an ensemble manner, we expect the ensemble network can overcome the prediction noise and class bias in the original label embeddings to gain robust zero-shot predictions. Moreover, we exploit the unlabeled data from unseen classes in an iterative self-training framework to overcome the domain shift problem. In each iteration, we select the most confidently predicted unlabeled instances from each unseen class under the current ensemble network, and combine these selected instances and their predicted pseudo-labels with the original seen class labeled data together to refine the ensemble network parameters, especially its feature extraction component. By incorporating the unseen class instances into the ensemble network training and dynamically refine the selected instances in each iteration, we expect the self-training process can effectively avoid overfitting to the seen classes and improve the generalization ability of the ensemble network on unseen classes. With the ensemble network directly handles multi-class classification over all classes, the proposed approach can be conveniently extended to address generalized ZSL. We conduct experiments on three standard ZSL datasets under both conventional ZSL and generalized ZSL settings. The empirical results demonstrate the proposed approach outperforms the state-of-the-art ZSL methods.

2 Related Work

2.1 Zero-Shot Learning

Deploying label embeddings in a common semantic space, e.g., visual attributes, to bridge the gap between seen and unseen classes is the key of ZSL. Existing ZSL methods have mostly been centered on learning a transferable mapping function between the input visual feature space and the semantic label space. ALE [1] and DeVISE [10] both use a linear projection to map visual features into the semantic space. LatEm [30] uses non-linear compatibility functions to match the two spaces, while some other works learn bilinear compatibility functions by minimizing a structural loss [2] or a squared loss [23]. Neural networks are used in [32, 3] to embed semantic information, while Semantic Auto-Encoders (SAE) with reconstruction loss is used in [27, 19] to learn better projections to the semantic space. SynC [7] and ConSE [21] embed unseen instances as a linear combination of seen class embeddings.

Despite the differences in embedding techniques, these methods are trained only on seen classes and have no clue about the visual appearance variations in unseen classes. They suffer from the aforementioned domain shift problem. Some most recent advances try to solve ZSL in a generative style. The work in [8] uses a linear projection to map an unseen semantic attribute vector into a visual feature space, which can be used for generating instances of the unseen classes. The work of [6] uses a generative moment matching network to generate unseen class instances, on which a classifier is directly trained for classification. In [34] the authors used a GAN to synthesize visual features from noisy texts. However the generated features in these works are not guaranteed to align well with the true unseen visual features, and can still suffer from the domain shift problem.

2.2 Transductive Zero-Shot Learning

Different from the standard zero-shot learning setting where unlabeled instances from unseen classes are treated as inaccessible in the training phase, transductive ZSL refers to the setting that unseen class instances are available during training. As none of the unseen class instances are labeled, this setting does not violate the ‘zero-shot’ principle. The existing transductive ZSL works have focused on improving standard ZSL by exploiting the unseen class instances to overcome the domain shift problem. In [12] the authors adopted a two-step procedure. They first used CCA to project both visual feature and class prototypes into a multi-view embedding space, and then used test instances

to build a hypergraph in the embedded space, on which label propagation is performed for image recognition. The authors of [18] proposed to solve ZSL from the viewpoint of unsupervised domain adaptation with sparse coding. They first learned a source semantic dictionary on seen classes, and then used it to regularize the learning of target semantic dictionary on unseen instances. In [14] the authors proposed to learn a shared model space on seen and unseen data to facilitate knowledge transfer between classes. More recently, the work in [27] uses auto-encoders and a maximum mean discrepancy loss to learn joint embeddings of visual and semantic vectors. It exploits unseen class instances to minimize a prediction loss for better adaptation. Last but not least, the work in [13] proposes to assign pseudo-labels to test instances and train embedding matrix on both seen and unseen class data. It nevertheless uses a single projection matrix to project visual features into the semantic space.

Our proposed work belongs to transductive zero-shot learning, but differs from the existing transductive ZSL works in two major aspects: (1) Instead of using one set of label embeddings that are not optimized for any target unseen class, our ensemble network uses multiple sets of label embeddings, each of which is produced by optimizing the inter-label relations between the seen classes and a subset of unseen classes. An ensemble combination of multiple classification functions with different output representations can facilitate robust knowledge transfer to all the unseen classes. (2) We use a self-training framework to incorporate a subset of unlabeled instances selected from the unseen classes and their predicted pseudo-labels to iteratively improve the ensemble network and prevent domain shift. In each iteration, with our dynamic instance selection procedure, new instances can be selected and previous ones might be dropped, which provides the ability to ‘correct’ potential bad predictions in previous iterations of self-training.

2.3 Self-Training with Pseudo-Labels

Exploiting unlabeled data by assigning them predicted pseudo-labels in a self-training procedure has been deployed in standard classification settings in the literature. A notable example is the well-known co-training method [4], which uses two different classifiers to produce pseudo-labels on unlabelled data. This method has been applied to different tasks, including sentiment classification [29], and domain adaptation [9]. Sharing similar ideas with co-training, a recent Tri-training method [33] also exploited outputs of three different classifiers. In [25], the authors applied tri-training in solving unsupervised domain adaptation problems. Distinct from these works above, our proposed work proposes a novel ensemble network that contains multiple classification functions with different label embeddings to address a more challenging zero-shot learning problem using a self-training procedure.

3 Approach

We consider zero-shot image recognition in the following setting. We have a set of N^s labeled images, $\mathcal{D}_s = \{(x_i, y_i)\}_{i=1}^{N^s}$, from L^s seen classes $\mathcal{S} = \{1, \dots, L^s\}$ such that $y_i \in \mathcal{S}$. We also have a set of N^u images, $\mathcal{D}_u = \{(x_j, y_j)\}_{j=1}^{N^u}$, from L^u unseen classes $\mathcal{U} = \{L^s + 1, \dots, L\}$ such that $L = L^s + L^u$, where the labels, $\{y_j \in \mathcal{U}\}$, are unavailable during training. We aim to transfer information from the labeled data to predict the labels of the unlabeled instances. To bridge the gap between seen and unseen classes, we also assume we have a semantic label representation matrix $M \in \mathbb{R}^{m \times L}$, e.g., semantic attribute vectors, for all the L seen and unseen classes.

In this section, we present a novel self-training ensemble network model for zero-shot image recognition. The proposed framework is depicted in Figure 1. It consists of multiple image classification functions with a shared feature extraction network but different label embedding representations, which perform zero-shot prediction in an ensemble manner. A self-training framework is deployed to iteratively refine the overall ensemble network by incorporating unlabeled instances with their predicted pseudo-labels. In what follows, we present the proposed model in detail.

3.1 Ensemble Networks

Following the standard ZSL scheme, we can use a convolutional neural network (CNN) f_v to extract high level visual features from an image x , and then use an embedding network f to embed the visual features $f_v(x)$ into the semantic space, e.g., the attribute space, of label embeddings \mathbb{R}^m . Here the overall deep network $f \circ f_v(x)$ (“ \circ ” denotes a composition operation) forms an image

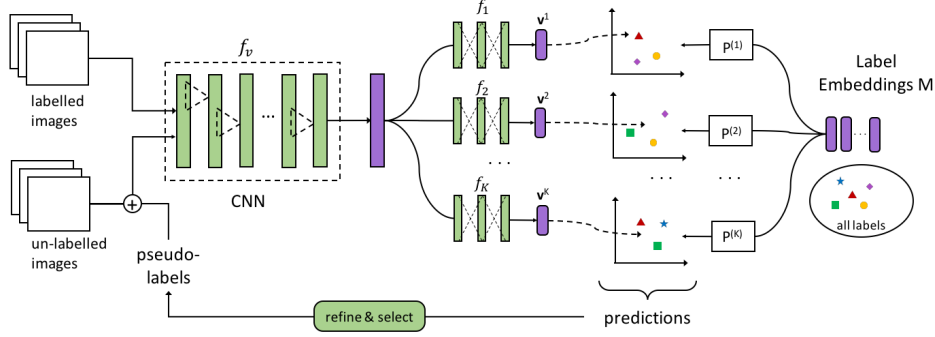


Figure 1: The proposed ensemble network based self-training framework for zero-shot learning. The ensemble network consists of multiple (K) image classification functions, each of which is a composition of a shared image feature extraction function f_v and an individual semantic embedding function f_k , i.e., $f_k \circ f_v(x)$, with $k \in \{1, \dots, K\}$. We use the ResNet-34 [15] as the feature extraction convolutional neural network f_v and use a multilayer perceptron with two hidden layers (512 units) and ReLU activation functions as each embedding function f_k . Self-training is an iterative training procedure, which dynamically selects unlabeled instances from unseen classes and their predicted pseudo-labels in each iteration to augment the training data and refine the ensemble network.

classification function for all classes, $\mathcal{S} \cup \mathcal{U}$, which can categorize an image x to the nearest class in the semantic label embedding space \mathbb{R}^m . However, though a semantic label embedding matrix M can enable zero-shot information transfer from the seen classes to the unseen classes, the effectiveness of such information transfer can vary substantially for different unseen classes due to their various association levels with the seen classes in the given semantic label embedding space. It is hard to optimize the semantic associations of the seen classes with all unseen classes simultaneously, while preserving the inter-class distinctions across the unseen classes, with one fixed label embedding matrix M . Hence we propose to project the label embeddings M into K different embedding spaces, $\{\mathcal{P}_k : \mathbb{R}^m \rightarrow \mathbb{R}^h \mid k = 1, \dots, K\}$, to induce K sets of different label embeddings $\{\mathcal{P}_k(M)\}$ to facilitate information transfer to different unseen classes. For each label embedding matrix $\mathcal{P}_k(M)$, we can produce an embedding network f_k to map $f_v(x)$ into the corresponding label embedding space, which forms a zero-shot classification function $f_k \circ f_v(x)$. By employing the K classification functions in an ensemble manner we expect the overall ensemble network can effectively reduce the impact of noise and class bias of the original label embeddings M to produce robust zero-shot image recognitions.

3.1.1 Label Embedding Projection

We aim to use different label embeddings to capture different label associations between seen and unseen classes. Towards this goal, we perform the k -th label embedding projection \mathcal{P}_k by maximizing the similarity score between the seen classes, \mathcal{S} , and a randomly selected subset of the unseen classes, $\mathcal{Z}_k \subset \mathcal{U}$, in the projected label embedding space. In particular, we assume a linear projection function $\mathcal{P}_k(M) = P^{(k)}M$, where the projection matrix $P^{(k)} \in \mathbb{R}^{h \times m}$ ($h < m$) has orthogonal rows, i.e., $P^{(k)}P^{(k)\top} = I$. We formulate the label embedding projection as the following maximization problem:

$$\max_{P^{(k)}} \sum_{i \in \mathcal{S}, j \in \mathcal{Z}_k} \text{tr}(P^{(k)}M_{:i}M_{:j}^\top P^{(k)\top}) \quad \text{subject to} \quad P^{(k)}P^{(k)\top} = I \quad (1)$$

where $M_{:i}$ denotes the i -th column of matrix M and $\text{tr}(\cdot)$ denotes a trace function. This maximization problem has a closed-form solution:

$$P^{(k)} = [\mathbf{u}_1, \mathbf{u}_2, \dots, \mathbf{u}_h]^\top \quad (2)$$

where $\{\mathbf{u}_i\}_{i=1}^h$ are the top h eigenvectors of matrix $\sum_{i \in \mathcal{S}, j \in \mathcal{Z}_k} \frac{1}{2}(M_{:i}M_{:j}^\top + M_{:j}M_{:i}^\top)$.

We can produce K different label embedding projection matrices $\{P^{(k)}\}_{k=1}^K$ by randomly selecting K different subsets of unseen classes, $\{\mathcal{Z}_k\}_{k=1}^K$. Each resulting label embedding matrix $P^{(k)}M$ encodes a different knowledge transfer structure between the seen and unseen classes.

3.1.2 Ensemble Network Training

Given labeled training instances $\mathcal{D}_{train} = \{(x_i, y_i)\}_{i=1}^N$, the deep ensemble neural network with K classification functions, $\{f_k \circ f_v(x)\}_{k=1}^K$, can be trained by minimizing the following negative log-likelihood loss function:

$$\mathcal{L}(\omega_v, \omega_1, \dots, \omega_K) = \frac{1}{N} \sum_{i=1}^N \sum_{k=1}^K \ell_k(\mathbf{v}_i^k, y_i) \quad (3)$$

where $(\omega_v, \omega_1, \dots, \omega_K)$ denote the model parameters, $\mathbf{v}_i^k = f_k \circ f_v(x_i)$ denotes the k -th classifier's prediction vector of instance x_i in its label embedding space, and $\ell_k(\cdot, \cdot)$ is a negative log-likelihood loss function computed over the softmax prediction scores of the k -th classifier:

$$\ell_k(\mathbf{v}_i^k, c) = -\log p_k(c|\mathbf{v}_i^k) = -\log \frac{\exp(\mathbf{v}_i^{k\top} P^{(k)} M_{:c})}{\sum_{c' \in \mathcal{S} \cup \mathcal{U}} \exp(\mathbf{v}_i^{k\top} P^{(k)} M_{:c'})} \quad (4)$$

We adopted the Adam algorithm [17] to perform training. Note the softmax function above is defined over both seen and unseen classes. It is designed to include training instances from both seen and unseen classes. Hence, although initially the labeled training data only contain the labeled instances from the seen classes, such that $\mathcal{D}_{train} = \mathcal{D}_s$ and $N = N^s$, we will expand it to include pseudo-labeled set from unseen classes through self-training below.

3.1.3 Ensemble Zero-Shot Prediction

With the multiple classification functions learned in the ensemble network, we can integrate the K classification functions to perform zero-shot prediction on each unlabeled instance x_i from unseen classes. We first make predictions using each of the K classifiers based on similarity scores:

$$\hat{y}_i^{(k)} = \arg \max_{c \in \mathcal{Z}_k} \langle f_k \circ f_v(x_i), P^{(k)} M_{:c} \rangle \quad (5)$$

where $\langle \cdot, \cdot \rangle$ denotes the inner product of two vectors. As the k -th set of label embeddings are produced by maximizing the label associations of seen classes and the subset of unseen classes \mathcal{Z}_k , we hence only use the k -th classifier for zero-shot predictions on the subset of unseen classes \mathcal{Z}_k . Then we ensemble all the K predictions to determine the predicted class using a normalized majority voting strategy:

$$\hat{y}_i = \arg \max_c \phi(x_i, c) \quad (6)$$

$$\text{where } \phi(x_i, c) = \frac{\sum_{k=1}^K \mathbb{I}[c = \hat{y}_i^{(k)}]}{\sum_{k=1}^K \mathbb{I}[c \in \mathcal{Z}_k]} \quad (7)$$

and $\mathbb{I}[\cdot]$ denotes an indicator function that returns value 1 when the given condition is true.

In the case of generalized ZSL, where a test instance x_i can be from either a seen or an unseen class, we still compute the voting score of x_i belonging to an unseen class c using the normalized voting score in Eq.(7), but we compute the voting score of x_i belonging to a seen class c as its average prediction score on this class by all the K classifiers, i.e., $\phi(x_i, c) = \frac{1}{K} \sum_{k=1}^K \langle f_k \circ f_v(x_i), P^{(k)} M_{:c} \rangle$.

3.2 Self-Training Ensemble Networks

Training with only labeled instances from the seen classes can suffer from the aforementioned domain shift problem. Meanwhile our ensemble network provides a natural foundation for making voting-based predictions on the unseen class instances and incorporating pseudo-labeled instances from the unseen classes in the training process. We hence propose to deploy a self-training procedure that iteratively exploits pseudo-labeled unseen class instances to refine the ensemble network initially trained on the labeled data from seen classes, \mathcal{D}_s .

The self-training algorithm is summarized in Algorithm 1. In each iteration, it uses the current ensemble network to predict the pseudo-label \hat{y}_i with Equation (6) for each unlabeled instance x_i from the unseen classes. Then for each unseen class $c \in \mathcal{U}$, it selects the top N_{pseudo} instances with the largest prediction scores $\phi(x_i, c)$. The instances selected from all the unseen classes together

Algorithm 1 Self-Training Ensemble Networks with Pseudo-Labels

Input: labeled data from seen classes \mathcal{D}_s , unlabeled data from unseen classes \mathcal{D}_u ,
and label embedding matrix M .
Initialization: $\mathcal{D}_{train} \leftarrow \mathcal{D}_s$, $\mathcal{D}_{pseudo} \leftarrow \emptyset$;
perform label embedding projection for $\{P^{(k)}\}_{k=1}^K$;
train an end-to-end deep ensemble network on \mathcal{D}_{train} .
repeat
 predict pseudo-labels of \mathcal{D}_u by Eq.(6) and (7);
 generate a pseudo-labeled set \mathcal{D}_{pseudo} by selecting the top N_{pseudo} instances
 from each unseen class;
 update the training set: $\mathcal{D}_{train} \leftarrow \mathcal{D}_s \cup \mathcal{D}_{pseudo}$;
 refine the ensemble network parameters on \mathcal{D}_{train} .
until MaxIter

with their predicted labels form a pseudo-set $\mathcal{D}_{pseudo} = \{(x_i, \hat{y}_i)\}_{i=1}^{N_p}$. The ensemble network parameters are then refined by minimizing a loss function in Equation (3) over an augmented training set $\mathcal{D}_{train} = \mathcal{D}_s \cup \mathcal{D}_{pseudo}$. As the augmented training set contains data from both the seen classes and unseen classes, we expect the refined ensemble network can overcome the domain shift problem in terms of visual appearances of semantic features and improve zero-shot prediction performance. Moreover, instead of gradually increasing the pseudo-set, we dynamically update this set in each iteration with the iteratively improved ensemble network to correct potential label mistakes in the previous pseudo-set.

4 Experiments

To investigate the empirical performance of our proposed approach, we conducted experiments on multiple standard ZSL datasets by comparing our approach with the state-of-the-art methods. We first conducted experiments under the conventional ZSL setting and then investigated our approach under the generalized ZSL setting. In this section, we present our experimental results and discussions.

4.1 Experiment Settings

Datasets We used three widely used ZSL datasets with label attribute vectors for conducting experiments. The first one is the Caltech-UCSD-Birds 200-2011 (CUB) dataset [28]. It is a fine-grained dataset of bird species, containing 11,788 images of birds from 200 different species. Each image is also annotated with 312 attributes. The second one is the SUN dataset [22], which contains 14,340 images from 717 different scenes. In this dataset each image is annotated with 102 attributes. The third dataset is the Animal with Attributes 2 (AWA2) dataset [31], which is an updated version of previous AWA [20] dataset. AWA2 consists of 37,322 images from 50 animal classes. It also provides 85 numerical attribute values for each class. We used AWA2 instead of AWA as the raw image data of AWA is not publicly available any more. Following previous ZSL works, we extracted the label embedding matrix M from the attribute vectors on each dataset.

Seen/Unseen Splits In order to perform ZSL, the datasets need to be split into a set of seen classes \mathcal{S} and a set of unseen classes \mathcal{U} such that contain two disjoint sets of classes. To perform scientific ZSL study and maintain the ‘zero-shot’ principle, a ZSL model should never have access to the true label information of the unseen class instances during the training phase. However many ZSL approaches have used CNN models pre-trained on the ImageNet [24] for image feature extraction. If the pre-trained ImageNet classes have overlap with the ZSL test classes, i.e., the unseen classes, it should be considered as violating the ‘zero-shot’ rule. As pointed out by the comprehensive evaluation study in [31], standard splits (SS) on the ZSL datasets have various numbers of classes overlapping with the 1K classes of ImageNet, which can lead to superior performance on these classes. Therefore in this study we used the ZSL splits proposed in [31] (PS), which has the same number of test classes as the SS splits but ensures no class in ImageNet appears in the test set of ZSL. We also reported the results in SS splits for comparison purpose. The overview of these datasets and seen/unseen class splits is summarized in Table 1.

Table 1: Summary of three attribute datasets for ZSL.

DATASET	IMAGES	AVG.	CLASSES	ATTR.
CUB	11788	~ 60	200 (150+50)	312
SUN	14340	~ 20	717 (645+72)	102
AWA2	37322	~ 750	50 (40+10)	85

Table 2: Conventional ZSL results. \dagger denotes numbers cited from [31]. Methods in the top part of the table reported the Top-1 accuracy results (TOP-1), while those in the bottom part reported the multi-class accuracy (MACC) results. Numbers in bracket denote results on AWA instead of AWA2.

	METHODS	CUB		AWA2		SUN72		SUN10
		SS	PS	SS	PS	SS	PS	
TOP-1	DEViSE [10] \dagger	53.2	52.0	68.6	59.7	57.5	56.5	-
	SYNC [7] \dagger	54.1	55.6	71.2	46.6	59.1	56.3	-
	ALE [1] \dagger	53.2	54.9	80.3	62.5	59.1	58.1	-
	SJE [2] \dagger	55.3	53.9	69.5	61.9	57.1	53.7	-
	SAE [19] \dagger	33.4	33.3	80.7	54.1	42.4	40.3	-
	REViSE [27]	65.4	-	(93.4)	-	-	-	-
	SELF TRAINING	54.0	49.8	73.2	57.8	49.6	47.9	76.6
	STEN(PROPOSED)	67.0	65.7	95.0	75.2	63.9	62.0	88.7
MACC	UDA [18]	40.6	-	(75.6)	-	-	-	-
	DCL [13]	-	-	(81.9)	-	-	-	84.4
	SELF TRAINING	53.7	49.9	73.0	53.8	49.5	48.0	76.7
	STEN(PROPOSED)	66.7	65.6	95.3	77.4	63.8	62.0	88.7

Note that for the SUN dataset, except for the split with 72 test classes, there is another split with 10 test classes from [16], which is also used in some previous works. We denote this split as SUN10 and the split with 72 test classes as SUN72.

Evaluation Metric We mainly adopted the popularly used Top-1 accuracy to evaluate the ZSL prediction performance. The Top-1 accuracy counts the proportion of correctly labeled instances in each test class and then takes an average over all these classes. But to compare with some literature works, we also reported the multi-class classification accuracy results when needed.

Parameter Selection The proposed model has two hyperparameters: K , the number of classifiers (or label embeddings), and h , the dimension of projected class label embeddings. For a simpler parameter selection procedure, we compute h as a fraction of the original label embedding dimension m , i.e. $h = \lfloor \gamma \times m \rfloor$ with $\gamma \in (0, 1]$. We then selected K from $\{10, 20, \dots, 50\}$ and γ from $\{0.5, 0.6, \dots, 1.0\}$. We conducted parameter selection on the CUB training set, which is further split into 100 classes for training and 50 classes for validation, and then fixed the selected values across all the other datasets and experiments.

Implementation Details For an input image, we resized it to 224×224 and fed it to ResNet-34 [15]. The 512 dimensional vector from last average pooling layer of ResNet is connected to the embedding multilayer perceptrons (MLP) as visual features of the image. The ResNet is initialized by the pre-trained model on ImageNet. For the ensemble classifiers, we used MLP with two hidden layers of size 512 and one output layer of size h . Rectified Linear Unit (ReLU) is applied after each layer. We used Adam [17] to train our model, with the default parameter setting $\beta_1 = 0.9$, $\beta_2 = 0.999$ and learning rate $\eta = 0.001$. In each iteration the model is trained with 100 batches with a batch size of 64 and `MaxIter` = 20 is used for all experiments. For the self-training procedure, we used $N_{pseudo} = \min(\rho N_{avg}, N_{max})$, where N_{avg} is the average number of images in each training class, ρ and N_{max} are set to 0.25 and 20, respectively. For $\{\mathcal{Z}_k\}_{k=1}^K$, which are the randomly selected subsets of unseen classes for producing the label embedding projection matrices, we set the size of each \mathcal{Z}_k as half of the unseen class number and set $K = 50$.

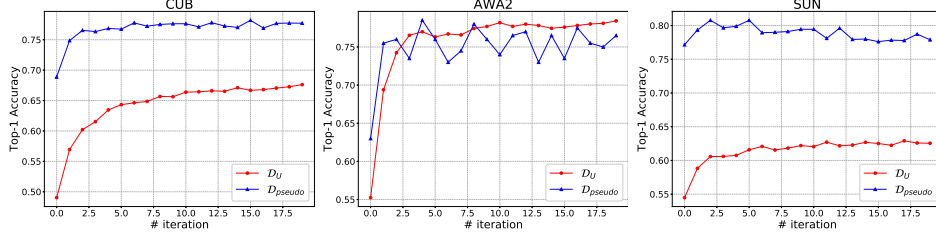


Figure 2: Test results vs # of self-training iterations for conventional ZSL on the three datasets CUB, AWA2 and SUN.

4.2 Conventional ZSL Results

Comparison Methods We compared our proposed Self-Training Ensemble Network (STEN) approach with a number of state-of-the-art ZSL methods. These methods can be divided into two groups. DeViSE [10], SynC [7], ALE [1], SJE [2], and SAE [19] belong to inductive ZSL methods, while the transductive methods include UDA [18], DCL [13] and ReViSE [27]. All the comparison methods used the standard fixed splits. We hence take convenience to cite the results for the inductive methods from [31] as it provided a comprehensive evaluation on these methods, which can provide fair comparisons with our proposed model. Moreover, in order to separate the impact of the self-training principle from our proposed ensemble framework, we also compared with a *Self-Training* baseline variant of the proposed model, which drops the ensemble framework to use only one classifier with an identity matrix for label embedding projection.

Results Analysis We summarized the comparison results in Table 3. As two different evaluation metrics, Top-1 Accuracy and multi-class accuracy, are used in the comparison works, we divide the table into two parts, where the top part presents Top-1 accuracy results and the bottom part presents multi-class accuracy results. We reported the results of our proposed STEN method in terms of both evaluation metrics. From the table, we notice that most results on ‘PS’ are worse than their counterpart results on ‘SS’, especially on the AWA2 datasets. This indicates that the overlapping of test classes with ImageNet 1K classes did bring extra benefit in performance, and it is better to use the ‘PS’ splits. However, the transductive ZSL methods we found are all evaluated under the ‘SS’ setting, we hence expect their missing results under ‘PS’ can only be worse than the reported ‘SS’ results. Moreover, the transductive works, ReViSE, UDA and DCL, reported results on CUB, AWA or SUN10, but not on AWA2 and SUN72. Since AWA2 is nearly a drop-in-replacement of AWA [31], we included their results on AWA just for reference.

From the comparison results in terms of Top-1 accuracy, we can see the best results reported on CUB, AWA2 and SUN72 with ‘PS’ splits by the comparison methods are 55.6%, 62.5%, and 58.1% respectively, while the proposed STEN achieves 65.7%, 75.2% and 62.0% respectively and greatly improved the zero-shot learning classification performance. STEN also outperforms the transductive ReViSE on the ‘SS’ split of CUB (67.0% vs 65.4%). In terms of multi-class accuracy, our proposed STEN again largely outperforms the two transductive ZSL methods, UDA and DCL. For example, STEN achieves 66.7% on CUB and 88.7% on SUN10, which are much better than the 40.6% reported by UDA on CUB and the 84.4% reported by DCL on SUN10 respectively. These results demonstrate the efficacy of the proposed STEN approach for conventional zero-shot image recognition tasks. Moreover, we notice there are large performance gaps between the proposed full model STEN and the Self-Training baseline variant. This shows that self-training alone will not produce an effective model and the proposed ensemble network architecture with label embedding projections forms a solid and critical foundation for incorporating pseudo-labels through a self-training procedure.

4.3 Effectiveness of Iterative Training

In this section we study the efficacy of iterative training procedure of the proposed model in incorporating instances with pseudo-labels. The main idea of the iterative self-training is to gradually improve the ZSL ensemble network by integrating a selected pseudo-set from unseen classes into the training data. With the improvement of ZSL performance, the model is expected to more accurately predict the pseudo-labels on \mathcal{D}_u and thus leads to a better pseudo-set \mathcal{D}_{pseudo} , which consequently

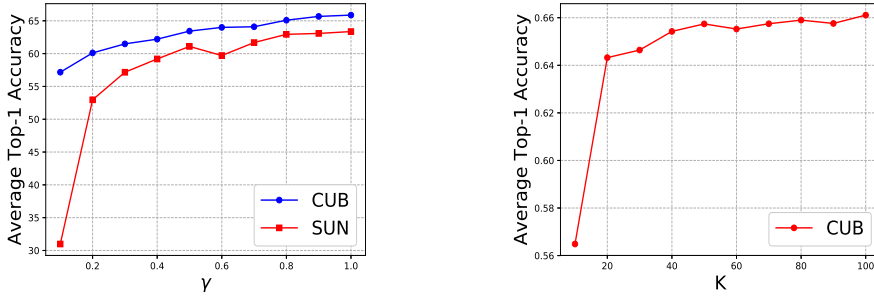


Figure 3: Parameter sensitivity analysis.

can further benefit the ZSL ensemble network in the following iteration. To verify whether this assumption holds in reality, we run experiments on all the three datasets, CUB, AWA2 and SUN, while in each self-training iteration we tested the prediction accuracy on the unlabeled instances from the unseen classes \mathcal{D}_u . We also computed the test accuracy on the selected pseudo-set \mathcal{D}_{pseudo} . We plot the test accuracies vs the self-training iterations in Figure 2.

From the results in the figure, we can have multiple observations. First, on CUB and SUN the test accuracy on \mathcal{D}_{pseudo} increases as the number of iteration increases, which suggests the model can select more accurate pseudo-set with the iterative self-training. Second, the accuracy on \mathcal{D}_{pseudo} is much higher than on the test set \mathcal{D}_u , which suggests our model is able to select the most confident subsets of instances. Last but not least, by augmenting the training data with the pseudo-set \mathcal{D}_{pseudo} , the model’s test accuracy on test set consistently increases with the iteration continuing. Even when the test accuracy on \mathcal{D}_{pseudo} vibrates (especially in AWA2), the increasing pattern of the test accuracy on \mathcal{D}_u does not change. This suggests our proposed model provides an effective self-training framework for ZSL. We also notice that on AWA2 the test performance on \mathcal{D}_u is very close to, some times even higher than, that on the selected pseudo instances. The reason is that AWA2 is a rather simple dataset with fewer target classes and many images per class. The model training on AWA2 is easier to converge into a state where it is equally certain about its predictions, regardless of being correct or wrong, on the instances, such that even the most confident predictions contain a similar fraction of wrong labels as all predictions. On the other hand, the model is trained on both \mathcal{D}_s and \mathcal{D}_{pseudo} , which makes it less sensitive to fluctuations in \mathcal{D}_{pseudo} .

4.4 Parameter Sensitivity Analysis

In this section, we investigate the sensitivity of the proposed model with respect to its two hyper-parameters, K and γ . K is the number of projected label embeddings as well as the number of classifiers, while γ determines the dimension of projected label embeddings by $h = \lfloor \gamma \times m \rfloor$.

To study how does γ affect the test performance, we performed conventional ZSL on the CUB and SUN72 datasets, with the ‘PS’ splits used. We fixed $K = 50$ and run the experiment 5 times for each γ from the set $\{0.1, 0.2, \dots, 1.0\}$. The average test accuracy over the 5 runs is reported on the left side of Figure 3. We can see that on both datasets, the test ZSL accuracies increase quickly before γ reaches 0.5, and then the increase becomes very small. Nevertheless the best performance is achieved at $\gamma = 1.0$. This suggests that larger dimension does help maximally preserve useful information in the projected label embeddings. But even with half of the original dimension, $\gamma = 0.5$, the performance is already very close to the best. We conclude that a γ value within $(0.5, 1.0]$ would be a safe choice for our model.

We also performed sensitivity analysis for K on the CUB dataset. We perform conventional ZSL on CUB, with γ fixed to 1.0 and K taking different values from $\{10, 20, \dots, 100\}$. For each K value, the experiment was run 5 times and we reported the average of test accuracy in the right subfigure of Figure 3. It is easy to observe that the ZSL accuracy is very poor when K has a small value 10. Then the ZSL performance dramatically increases with K increases from 10 to 40, and does not change much any more from the further increasing of K to 100. These results suggest our proposed model is not very sensitive to the hyper-parameters K and γ as long as they are set to values within the reasonable range, such as $\gamma \in (0.5, 1]$ and $K \geq 40$.

Table 3: Generalized ZSL results in terms of average Top-1 accuracy. † denotes numbers cited from [31]. ‘u’ and ‘s’ denotes Top-1 accuracies on unseen and seen classes, respectively. ‘H’ denotes the harmonic mean of them.

METHODS	CUB			AWA2			SUN72		
	U	S	H	U	S	H	U	S	H
DEVISE [10]†	23.8	53.0	32.8	17.1	74.7	27.8	16.9	27.4	20.9
SYNC [7]†	11.5	70.9	19.8	10.0	90.5	18.0	7.9	43.3	13.4
ALE [1]†	23.7	62.8	34.4	16.8	76.1	27.5	21.8	33.1	26.3
SJE [2]†	23.5	59.2	33.6	8.0	73.9	14.4	14.7	30.5	19.8
SAE [19]†	7.8	54.0	13.6	1.1	82.2	2.2	8.8	18.0	11.8
STEN(PROPOSED)	39.4	51.5	44.7	40.7	87.8	55.6	29.6	33.1	31.1

4.5 Generalized ZSL Results

Majority of ZSL works in the literature has focused on the conventional ZSL setting, where the test classes are assumed to consist of only unseen classes. This assumption can be overly strict. Hence here we conducted experiments to compare the test performance of the proposed self-training ensemble network (STEN) with related methods under the generalized ZSL (GZSL) setting, where the test instances can come from both seen and unseen classes. As the classifiers within our STEN model perform multi-class classification over all the classes, it can be conveniently extended to address GZSL. For GZSL the main problem is that many unseen class instances can be wrongly classified into seen classes. Hence we only select pseudo instances for unseen classes in the first few iterations of the self-training process, while selecting pseudo instances for both seen and unseen classes in later iterations to achieve balanced performance. To evaluate our model under GZSL, we follow the comprehensive study in [31] to use the ‘PS’ splits, and separate a random 20% of the instances for each seen class and add these into the test set. Follow [31], we evaluated the top-1 test accuracy on unseen and seen classes separately, and compute their harmonic mean as the GZSL accuracy result. We compared with four ZSL methods that have addressed GZSL in the literature. The comparison results are reported in Table 3.

We can see that some comparison methods can achieve quite good performance on seen classes while their zero-shot accuracy on unseen classes is very low; for example SynC achieves 11.5% (unseen) and 70.9% (seen) on AWA2, as well as 10.0% (unseen) and 90.5% (seen) on CUB. The overall performance of the comparison methods on all classes, under column ‘H’, is still poor. We also notice there is usually a trade-off between the performance on the seen classes and that on the unseen classes, while the harmonic mean measures the overall performance. The proposed STEN though didn’t yield superior performance on seen classes, its zero-shot prediction performance on *unseen* classes is much better than the other comparison methods. Moreover, in terms of the overall GZSL performance, we can see the proposed STEN outperforms all the comparison methods with large margins by achieving 44.7%, 55.6% and 31.1% GZSL accuracy on CUB, AWA2, and SUN72, respectively. This validates the effectiveness of the proposed model under GZSL setting.

5 Conclusion

In this paper, we proposed a novel self-training deep ensemble network for transductive zero-shot image recognition. By integrating multiple classifiers with different label embeddings, the ensemble network can maintain informative knowledge transfer from seen classes to unseen classes through optimized inter-label relations. By iteratively refining the ensemble network parameters with pseudo-labeled test instances, the self-training procedure can alleviate the domain shift problem and avoid overfitting to the seen classes. We conducted experiments on multiple standard datasets under both conventional ZSL and generalized ZSL settings. The proposed model has demonstrated superior performance than the state-of-the-art comparison methods.

References

- [1] Z. Akata, F. Perronnin, Z. Harchaoui, and C. Schmid. Label-embedding for attribute-based classification. In *CVPR*, 2013.
- [2] Z. Akata, S. Reed, D. Walter, H. Lee, and B. Schiele. Evaluation of output embeddings for fine-grained image classification. In *CVPR*, 2015.
- [3] J. Ba, K. Swersky, S. Fidler, et al. Predicting deep zero-shot convolutional neural networks using textual descriptions. In *ICCV*, 2015.
- [4] A. Blum and T. Mitchell. Combining labeled and unlabeled data with co-training. In *COLT*, 1998.
- [5] M. Bucher, S. Herbin, and F. Jurie. Improving semantic embedding consistency by metric learning for zero-shot classification. In *ECCV*, 2016.
- [6] M. Bucher, S. Herbin, and F. Jurie. Generating visual representations for zero-shot classification. In *ICCV Workshops: TASK-CV: Transferring and Adapting Source Knowledge in Computer Vision*, 2017.
- [7] S. Changpinyo, W.-L. Chao, B. Gong, and F. Sha. Synthesized classifiers for zero-shot learning. In *CVPR*, 2016.
- [8] S. Changpinyo, W.-L. Chao, and F. Sha. Predicting visual exemplars of unseen classes for zero-shot learning. In *ICCV*, 2017.
- [9] M. Chen, K. Q Weinberger, and J. Blitzer. Co-training for domain adaptation. In *NIPS*, 2011.
- [10] A. Frome, G. S Corrado, J. Shlens, S. Bengio, J. Dean, T. Mikolov, et al. Devise: A deep visual-semantic embedding model. In *NIPS*, 2013.
- [11] Y. Fu, T. M Hospedales, T. Xiang, and S. Gong. Transductive multi-view zero-shot learning. *IEEE TPAMI*, 37(11):2332–2345, 2015.
- [12] Y. Fu, T. M Hospedales, T. Xiang, and S. Gong. Transductive multi-view zero-shot learning. *TPAMI*, 37(11):2332–2345, 2015.
- [13] Y. Guo, G. Ding, J. Han, and Y. Gao. Zero-shot recognition via direct classifier learning with transferred samples and pseudo labels. In *AAAI*, 2017.
- [14] Y. Guo, G. Ding, X. Jin, and J. Wang. Transductive zero-shot recognition via shared model space learning. In *AAAI*, 2016.
- [15] K. He, X. Zhang, S. Ren, and J. Sun. Deep residual learning for image recognition. In *CVPR*, 2016.
- [16] D. Jayaraman and K. Grauman. Zero-shot recognition with unreliable attributes. In *NIPS*, 2014.
- [17] D. P Kingma and J. Ba. Adam: A method for stochastic optimization. In *ICLR*, 2015.
- [18] E. Kodirov, T. Xiang, Z. Fu, and S. Gong. Unsupervised domain adaptation for zero-shot learning. In *CVPR*, 2015.
- [19] E. Kodirov, T. Xiang, and S. Gong. Semantic autoencoder for zero-shot learning. In *CVPR*, 2017.
- [20] C. H Lampert, H. Nickisch, and S. Harmeling. Learning to detect unseen object classes by between-class attribute transfer. In *CVPR*, 2009.
- [21] M. Norouzi, T. Mikolov, S. Bengio, Y. Singer, J. Shlens, A. Frome, G. S Corrado, and J. Dean. Zero-shot learning by convex combination of semantic embeddings. In *ICLR*, 2014.
- [22] G. Patterson, C. Xu, H. Su, and J. Hays. The sun attribute database: Beyond categories for deeper scene understanding. *IJCV*, 108(1-2):59–81, 2014.
- [23] B. Romera-Paredes and P. HS Torr. An embarrassingly simple approach to zero-shot learning. In *ICML*, 2015.
- [24] O. Russakovsky, J. Deng, H. Su, J. Krause, S. Satheesh, S. Ma, Z. Huang, A. Karpathy, A. Khosla, M. Bernstein, A. C. Berg, and Li F.-F. ImageNet Large Scale Visual Recognition Challenge. *IJCV*, 115(3):211–252, 2015.
- [25] K. Saito, Y. Ushiku, and T. Harada. Asymmetric tri-training for unsupervised domain adaptation. In *ICML*, 2017.

- [26] R. Socher, M. Ganjoo, C. D Manning, and A. Ng. Zero-shot learning through cross-modal transfer. In *NIPS*, 2013.
- [27] Y.-H. Hubert Tsai, L.-K. Huang, and R. Salakhutdinov. Learning robust visual-semantic embeddings. In *ICCV*, 2017.
- [28] C. Wah, S. Branson, P. Welinder, P. Perona, and S. Belongie. The Caltech-UCSD Birds-200-2011 Dataset. Technical Report CNS-TR-2011-001, California Institute of Technology, 2011.
- [29] X. Wan. Co-training for cross-lingual sentiment classification. In *ACL*, 2009.
- [30] Y. Xian, Z. Akata, G. Sharma, Q. Nguyen, M. Hein, and B. Schiele. Latent embeddings for zero-shot classification. In *CVPR*, 2016.
- [31] Y. Xian, C. H Lampert, B. Schiele, and Z. Akata. Zero-shot learning-a comprehensive evaluation of the good, the bad and the ugly. *arXiv preprint arXiv:1707.00600*, 2017.
- [32] L. Zhang, T. Xiang, and S. Gong. Learning a deep embedding model for zero-shot learning. In *CVPR*, 2017.
- [33] Z.-H. Zhou and M. Li. Tri-training: Exploiting unlabeled data using three classifiers. *IEEE TKDE*, 17(11):1529–1541, 2005.
- [34] Y. Zhu, M. Elhoseiny, B. Liu, and A. Elgammal. Imagine it for me: Generative adversarial approach for zero-shot learning from noisy texts. *arXiv preprint arXiv:1712.01381*, 2017.